Available online at www.sciencedirect.com
ScienceDirect
Thin Solid Films 515 (2007) 6103–6106
www.elsevier.com/locate/tsf

# Analysis of CdS/CdTe devices incorporating a ZnTe:Cu/Ti Contact ☆

T.A. Gessert *, S. Asher, S. Johnston, M. Young, P. Dippo, C. Corwine

*National Renewable Energy Laboratory, 1617 Cole Blvd, Golden, Colorado 80401, USA*

Available online 1 February 2007

**Abstract**

High-performance CdS/CdTe photovoltaic devices can be produced using a ZnTe:Cu/Ti back contact deposited onto the CdTe layer. We observe that prolonged exposure of the ZnTe:Cu and Ti sputtering targets to an oxygen-containing plasma significantly reduces device open-circuit voltage and fill factor. High-resolution compositional analysis of these devices reveals that Cu concentration in the CdTe and CdS layers is lower for devices with poor performance. Capacitance–voltage analysis and related numerical simulations indicate that the net acceptor concentration in the CdTe is also lower for devices with poor performance. Photoluminescence analyses of the junction region reveal that the intensity of a luminescent peak associated with a defect complex involving interstitial Cu ($Cu_i$) and oxygen on Te ($O_{Te}$) is reduced in devices with poor performance. Combined with thermodynamic considerations, these results suggest that oxygen incorporation into the ZnTe:Cu sputtering target reduces the ability of sputtered ZnTe:Cu film to diffuse Cu into the CdTe.


## 1. Introduction

CdS/CdTe thin-film photovoltaic devices with fill factors approaching 77% have been demonstrated by incorporating a Cu-doped ZnTe contact interface layer between the CdTe absorber and a Ti outer metallization [1]. This contacting process uses ion-beam milling to establish a nearly stoichiometric CdTe surface prior to depositing ZnTe:Cu and Ti. The continuous valence bands at the CdTe/ZnTe:Cu interface, high net acceptor concentration ($N_A - N_D$) of ZnTe:Cu, and beneficial reactions between ZnTe:Cu and Ti can combine to yield devices with nearly ideal behavior (i.e., light/dark current–voltage [LIV/DIV] performance shows very little “crossover” or “rollover”) [2]. The high-temperature ZnTe:Cu/Ti contacting process also allows Cu to diffuse into the CdTe from the ZnTe:Cu layer. Concurrently, $N_A - N_D$ in the CdTe layer increases and the depletion width ($W_d$) of the device decreases [3]. Optimum LIV performance is attained when the amount of Cu entering the CdS layer is minimized, and $W_d$ is narrow enough to produce a high drift field in the CdTe absorber but still wide enough to limit effects of voltage-dependent collection.

The above description closely links Cu diffusion from the ZnTe:Cu layer to electrical changes in the CdTe layer. It follows that device performance should be controlled primarily by the contacting temperature and Cu availability (i.e., Cu concentration in ZnTe:Cu and/or the layer thickness). However, recent observations indicate that oxygen impurity within the ZnTe:Cu sputtering target can reduce the ability of the ZnTe:Cu layer to source Cu and thereby affect the resultant device performance. Understanding this type of interaction may provide insight into role(s) of oxygen during both the CdTe deposition and subsequent contact processing.

## 2. Experimental

The vapor-transport deposited (VTD) CdS/CdTe material and contacting processes used in this study were similar to that discussed previously [4]. The main difference is that the ZnTe:Cu/Ti contacts were formed after the ZnTe:Cu and Ti sputtering targets were exposed to an oxygen plasma used for reactive r.f. sputtering of ZnO:Al for about 500 h. The ZnTe:Cu/Ti contact was produced using ion-beam milling with Ar, sputter deposition of ZnTe:Cu (0.5-μm-thick film), and Ti (0.5-μm-thick film) contact layers at temperatures of 320 °C [3]. Light and dark current–voltage (LIV/DIV) measurements were

☆ This work has been authored by an employee or employees of the Midwest Research Institute under Contract No. DE-AC36-99GO10337 with the U.S. Department of Energy. The United States Government retains and the publisher, by accepting the article for publication, acknowledges that the United States Government retains a non-exclusive, paid-up, irrevocable, worldwide license to publish or reproduce the published form of this work, or allow others to do so, for United States Government purposes.
* Corresponding author.
*E-mail address:* tim_gessert@nrel.gov (T.A. Gessert).

0040-6090/$ - see front matter © 2007 Published by Elsevier B.V.
doi:10.1016/j.tsf.2006.12.107

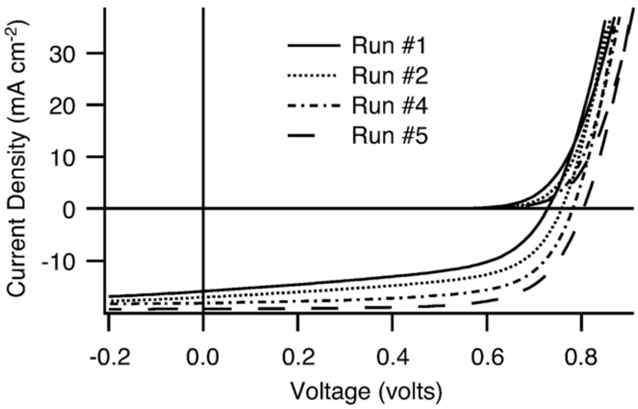


Fig. 1. LIV/DIV of CdS/CdTe material contacted with ZnTe:Cu/Ti at 320 °C as a function of number of runs following target exposure to the oxygen plasma.

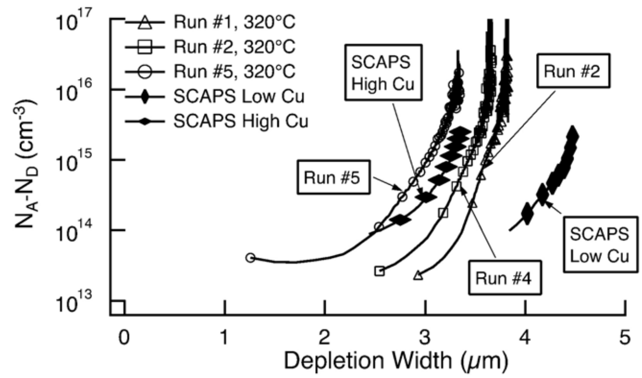


Fig. 3. Net acceptor concentration vs. depletion width as calculated from $C$–$V$ measurement (−8.0 V to 0.5 V) assuming an abrupt-junction model. Location of arrow from tag indicated depletion width at zero bias. Figure also shows SCAPS-1D simulation for the voltage range of −1.7 V to 0.5 V.

performed at room temperature using an XT-10 solar simulator adjusted to approximate Global AM1.5 current from a CdS/CdTe reference cell. Capacitance–voltage ($C$–$V$) measurements were performed in the dark using an HP 4274 LCR meter at a frequency of 100 kHz and a voltage bias range of +0.5 V to −8.0 V. Following chemical removal of the Ti layer, secondary ion mass spectrometry (SIMS) was performed from the contacted side of the devices using a Cameca IMS-3F instrument tuned for a mass resolution ($M/\Delta M$) of ~4000 to allow for separation of $^{63}Cu^{+}$ from $^{126}Te^{2+}$ species. Photoluminescence was performed at 4.25 K using an excitation frequency and power of 632.9 nm and 1 mW, respectively.

## 3. Results

Fig. 1 shows that the LIV/DIV characteristics of CdS/CdTe/ZnTe:Cu/Ti devices improve as a function of the number of contact depositions following exposure of the sputter targets to an oxygen-containing plasma ambient. The LIV performance

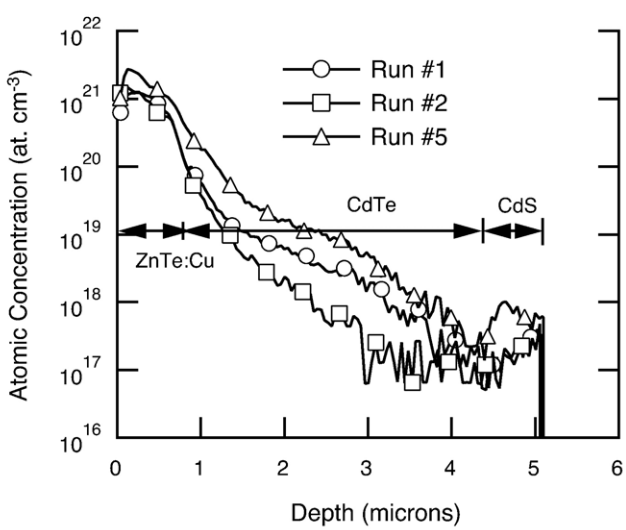


Fig. 2. Quantified high-resolution SIMS analysis of Cu (positive ion spectrum, oxygen beam) performed from ZnTe:Cu side of device.

for the best devices in this set (i.e., all devices produced after the fourth run) is typical of "good" baseline devices produced for this contact process on this CdS/CdTe material (e.g., 805 mV, 70% fill factor, and 19 mA cm$^{-3}$). Analysis of the DIV measurements indicates that the reverse saturation current density decreases systematically with increasing number of depositions, yielding the improvement of the LIV performance seen in Fig. 1.

Fig. 2 shows SIMS analysis for devices produced following progressive use of sputter targets. The analysis shows that contacts fabricated initially (Run #1 and #2, low target use) yield concentrations of Cu in both CdTe and CdS layers that previous studies have shown to produce devices with poor efficiency [2,3]. SIMS analysis was also performed to analyze the Na, Cl, and O concentration profiles in the ZnTe:Cu and CdTe layers. However, these studies have not revealed compositional trends that change systematically with progressive target use or device performance.

Fig. 3 shows $C$–$V$ analysis indicating that $N_A - N_D$ increases and $W_d$ reduces with the number of runs following oxygen exposure. These data support previous observations that Cu diffusion into the CdTe layer results in higher net acceptor concentration. The figure also compares results of simulated $C$–$V$ analysis of two simple device structures using SCAPS-1D (i.e., modeled structure is CdS/CdTe-1/CdTe-2/flat-band contact) [5]. In these simulations, only shallow donors or acceptors are considered for each layer (no deep defects). Also, because the valence band at the CdTe/ZnTe:Cu interface is continuous, and because the degenerate ZnTe:Cu produces a tunneling barrier with Ti, flat bands at the contact are assumed. Parameters used in the modeling are shown in Table 1, and parameters not indicated

Table 1
Parameters used for SCAPS-1D $C$–$V$ analysis simulations

| Model ID | CdS | CdS | CdTe-1 | CdTe-1 | CdTe-2 | CdTe-2 |
|---|---|---|---|---|---|---|
| | Thickness (μm) | $N_D$ (cm$^{-3}$) | Thickness (μm) | $N_A$ (cm$^{-3}$) | Thickness (μm) | $N_A$ (cm$^{-3}$) |
| Low Cu | 0.3 | 1e17 | 4.0 | 1e13 | 0.5 | 5e14 |
| High Cu | 0.3 | 1e15 | 3.0 | 3e13 | 1.5 | 5e15 |